Fibrous Nanomaterials

DOI: 10.1002/anie.201003451

High-Surface-Area Silica Nanospheres (KCC-1) with a Fibrous Morphology**

Vivek Polshettiwar, Dongkyu Cha, Xixiang Zhang, and Jean Marie Basset**

The past decade has seen significant advances in the ability to fabricate new porous solids with ordered structures from a wide range of different materials, with silica being the most common. Porous materials and their nanoscopic version now seem set to contribute to the developments in areas ranging from microelectronics to medical diagnosis or targeting of drugs.[1–4] The realm of mesoporous materials was extended after the emergence of Kresge's innovative method for the preparation of mesoporous silica materials (MCM-41) through the use of surfactants as organizing agents.[5] After the inception of template-directed synthesis of silica, extensive research was conducted to control their morphologies, pore sizes, and structures.[6–9] These templated techniques led to the synthesis of a variety of mesoporous and nanoscale silica materials with a wide range of morphologies[10–22] that have been successfully used as supports in heterogeneous catalysis.[23–30] The effectiveness of these materials as catalyst supports is mainly due to their microstructures, which allow active catalytic sites to disperse on the large internal surfaces and pores, which in turn improve the activity of the catalyst system. However, poor accessibility to these active sites inside the pores sometimes limits their applications for which significant mass transport is essential. Silica supports with easily accessible high surface areas (that is, not in the pores) are therefore needed. In quest of nanocatalysis[31] by surface organometallic chemistry (SOMC),[32,33] herein we present the synthesis of fibrous silica nanospheres (KCC-1) with high surface areas.[34] To the best of our knowledge, silica nanospheres with this type of fibrous morphology (Figures 1 and 2) is unprecedented. The high surface area is due to the presence of dendrimeric silica fibers and their respective channels, making KCC-1 a first-of-its-kind material.

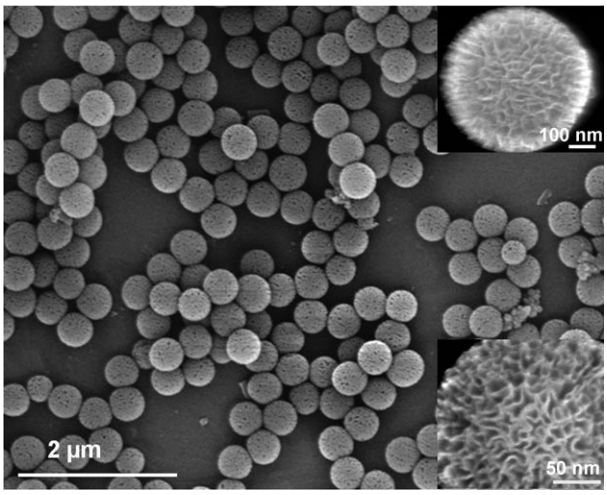

Figure 1. SEM images of silica nanospheres KCC-1.

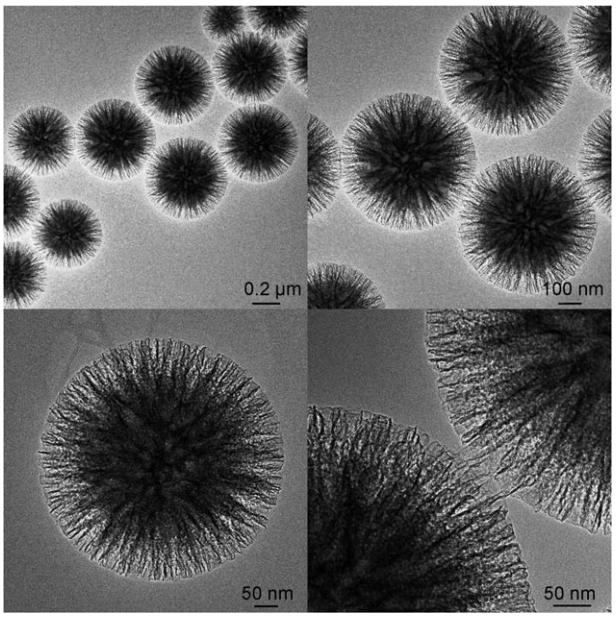

Figure 2. HRTEM images of silica nanospheres KCC-1.

KCC-1 can be readily prepared using the microwave-assisted hydrothermal technique in a short period of time. In a typical synthesis, tetraethyl orthosilicate (TEOS, 2.5 g, 0.012 mol) was dissolved in a solution of cyclohexane (30 mL) and pentanol (1.5 mL). A stirred solution of cetylpyridinium bromide (CPB; 1 g, 0.0026 mol) and urea (0.6 g,

[*] Dr. V. Polshettiwar, Prof. Dr. J. M. Basset
KAUST Catalysis Center (KCC)
King Abdullah University of Science and Technology, Thuwal (KSA)
E-mail: vivek.pol@kaust.edu.sa
jeanmarie.basset@kaust.edu.sa
Dr. D. Cha, Prof. Dr. X. Zhang
Advanced Nanofabrication
Imaging and Characterization Laboratory
King Abdullah University of Science and Technology, Thuwal (KSA)

[**] We are grateful to the KAUST nano-core laboratory group for their help in analysis of the silica spheres. We also thank Dr. V. Unkefer and Dr. T. McElwee for internal reviewing of the manuscript. Thanks are also due to Dr. J. Thivolle and Dr. L. Veyre of CPE, Lyon (France) for their help in mechanical stability study and surface area measurement, respectively. V.P. also thanks Dr. R. S. Varma for valuable comments on this work and Oak Ridge Institute for Science and Education (ORISE) for support during his stay at the US Environmental Protection Agency (US EPA), Cincinnati.

Supporting information for this article is available on the WWW under http://dx.doi.org/10.1002/anie.201003451.

0.01 mol) in water (30 mL) was then added. This mixture was stirred for 30 min at room temperature, and the resulting solution was placed in a Teflon-sealed microwave (MW) reactor. The reaction mixture was exposed to MW irradiation (400 W maximum power) at 120 °C for 4 h. After completion of the reaction, the mixture was allowed to cool to room temperature and the silica formed was isolated by centrifugation, washed with distilled water and acetone, and air-dried for 24 h. The as-synthesized material was then calcined at 550 °C for six hours in air.

Scanning electron microscopy (SEM) images (Figure 1) indicate that the material consists of colloidal spheres of uniform size with diameters that range from 250 nm to 450 nm. Close inspection of these images reveals that the material possesses dendrimeric fibers (angled with thicknesses of 8–10 nm) arranged in three dimensions to form spheres, which can allow easy access to the available high surface area. Further structural characterization of synthesized silica nanospheres performed by high-resolution transmission electron microscopy (HRTEM; Figure 2) reveals well-defined and ordered fibers coming out from the center of the particles and distributed uniformly in all directions.

Although SEM and HRTEM imaging of silica nanospheres indicates the presence of fibers, it was not clear whether these fibers grow from the center of the spheres or they are only on the surface of the silica spheres with solid cores inside. The three-dimensional (3D) tomography study of KCC-1 indicates that the fibers grow uniformly from the centers of the spheres along the free radial directions and the restricted tangential direction to form fibrous spherical silica particles (a video clip showing the results from the 3D tomography study is included in the Supporting Information).

Energy-dispersive X-ray spectroscopy (EDXS) analysis was utilized to determine the chemical composition of KCC-1 (Supporting Information, Figure S1). These results revealed that the material was composed of silicon and oxygen, thus confirming the formation of a silica material. Nearly similar percentages of silicon and oxygen were observed in the EDXS analysis of the edges and the central parts of the nanospheres. To verify the thermal stability, thermogravimetric analysis (TGA; Figure 3a) of the silica spheres was conducted in a nitrogen atmosphere. From room temperature to 1500 °C, only negligible weight loss up to about 3.8 % was observed. This weight loss could be attributed to the loss of chemically adsorbed water and hydroxy groups, as confirmed by TGA/Fourier-transform infrared (FTIR) analysis (Supporting Information, Figure S2). The material was also characterized by solid-state ^{29}Si cross-polarization magic-angle-spinning (CP-MAS) NMR spectroscopy. The resulting spectrum showed two characteristic signals at $\delta = -106$ and -112 ppm, which were assigned to the Q^3 and Q^4 sites corresponding to the SiO_4 substructures with different condensation degrees (Figure 3b). Absence of signals in the region around −60 indicated that no Si–C bonds are formed in the material. The nitrogen adsorption–desorption isotherms of the silica nanospheres made after the removal of the template by calcination exhibited the type IV pattern (Supporting Information, Figure S3). The Brunauer–Emmett–Teller (BET) surface area was found to be 641 $m^2 g^{-1}$.

The fabrication of KCC-1 fibrous nanosilica spheres involved microemulsion formation using cetylpyridinium bromide (CPB) or cetyltrimethylammonium bromide (CTB) as a template and urea in a mixture of cylcohexane, pentanol, and water. The silica precursor (TEOS) was hydrolyzed by urea, followed by assembly of hydrolyzed, negatively charged silicate molecules in the space available between the self-assembled template molecules (Figure 4) to aggregate along the free radial directions and the restricted tangential direction. Finally, condensation of self-assembled silicate led to the crystallization of the silica material within the isolated micelles (dispersed in the solvent), yielding fibrous silica nanospheres. However, the exact prediction of the shape and morphology of the silica remains a complex and yet unsolved problem.[35]

We observed that the fibrous morphology was lost when the template was changed to benzyldimethylhexadecyl ammonium chloride. This influence by the template molecules on the morphology is well-known and has been linked to the surfactant packing parameter, which depends upon the volume and length of the non-polar template chain (in this case cetyl) and also the effective area of the polar head (in this

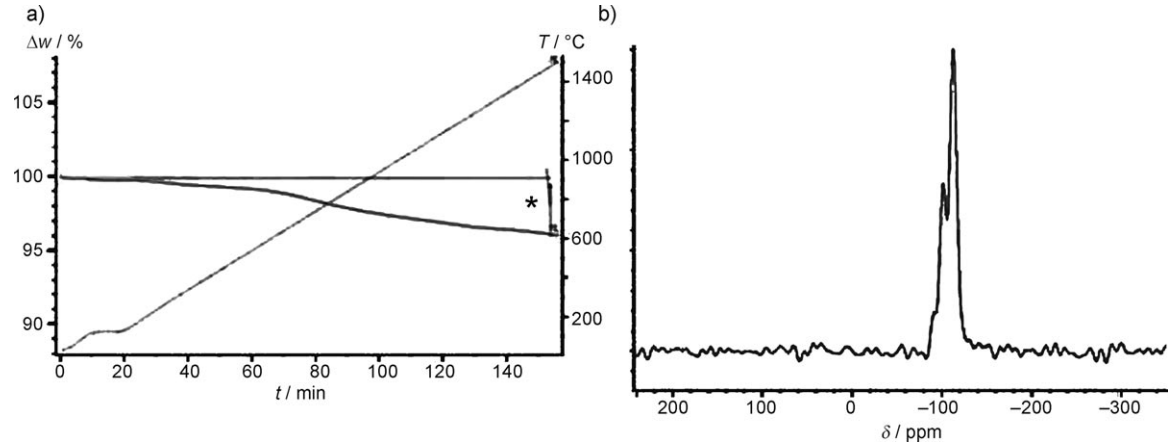

Figure 3. a) Thermal gravimetric analysis of KCC-1. ⋆ Mass change Δw of 3.8 %. b) ^{29}Si CP-MAS NMR spectrum of KCC-1.

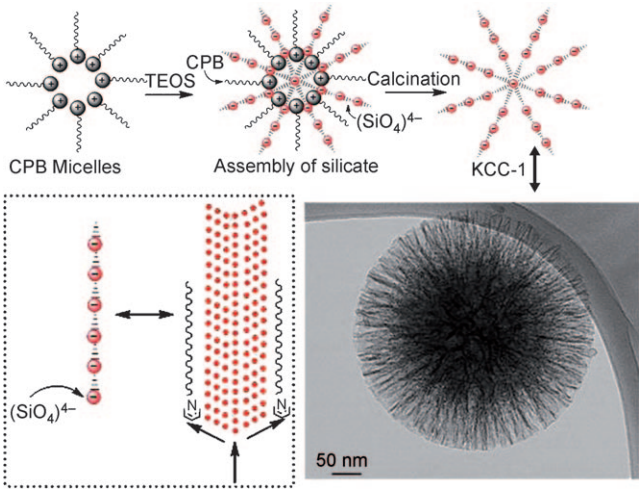

Figure 4. Schematic of silica nanosphere formation. CPB = cetylpyridinium bromide, TEOS = tetraethyl orthosilicate.

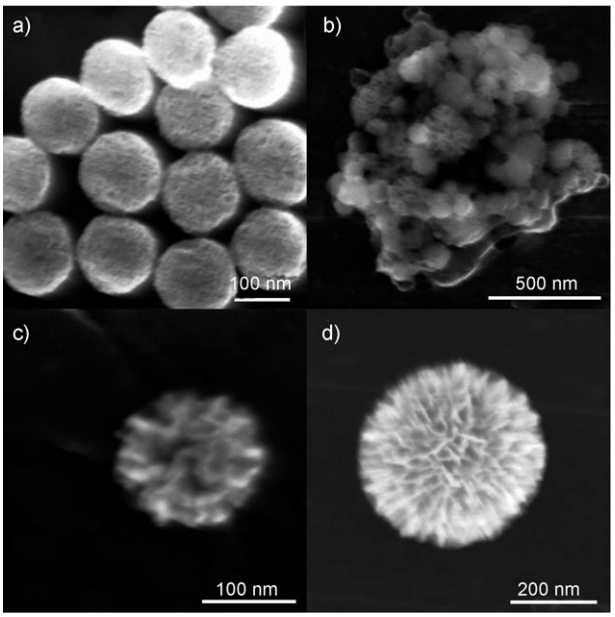

Figure 5. SEM images of silica nanospheres with a) 0.0, b) 0.003, c) 0.006, and d) 0.01 mol of urea per 0.012 mol of TEOS.

case pyridinium or trimethylammonium groups).[36] The morphology of the silica can also be affected by the organization of the surfactant molecules into a micellar liquid, which often precisely depends upon the delicate hydrophobic–hydrophilic equilibrium among the template, the precursor materials, the hydrolyzing reagent (in this case urea) and the solvents. To study the effect of the reaction solvent, several solvent combinations of cyclohexane and hexane with pentanol, butanol, or isopropanol were examined. Although silica spheres with fibrous morphologies were observed in all cases, the polydispersity varied strongly, leading to a particle size distribution between 50 nm and 200 nm. Thus, it appears that the mixture of cyclohexane and pentanol is a good combination of a solvent-yielding material with a narrow particle size distribution.

To study the effect of the urea concentration on the silica morphology, we conducted a series of experiments in which urea-to-TEOS molar ratios were varied. When no urea was used, only a small amount of silica was isolated, and the silica nanospheres were monodispersed with thin fibers as well as smaller sizes (90–120 nm; Figure 5a). These results indicate that the key to the fibrous morphology as well as particle size is the control on the speed of the TEOS hydrolysis by urea. This was also evident when silica synthesis with different amounts of urea was conducted. The SEM images shows that silica starts growing from none (Figure 5b) to poorly fibrous (Figure 5c) to highly fibrous (Figure 5d) nanospheres, when the concentration of the urea was increased from 0.18 gm (0.003 mol) up to 0.6 gm (0.01 mol). With a further increase in the amount of urea, no change in the fibrous morphology was observed except for an increase in the particle size distribution, which may be due to rapid (uncontrolled) hydrolysis of TEOS molecules by excess urea.

The SEM analysis (Figure 6) of KCC-1 at different temperatures (from 400 to 950 °C) indicated that silica nanospheres are thermally stable with no visible changes in the morphology and size of the particles. We did not observe any coalescence of particles even after severe thermal treatment. This is an interesting observation, as thermal stability is

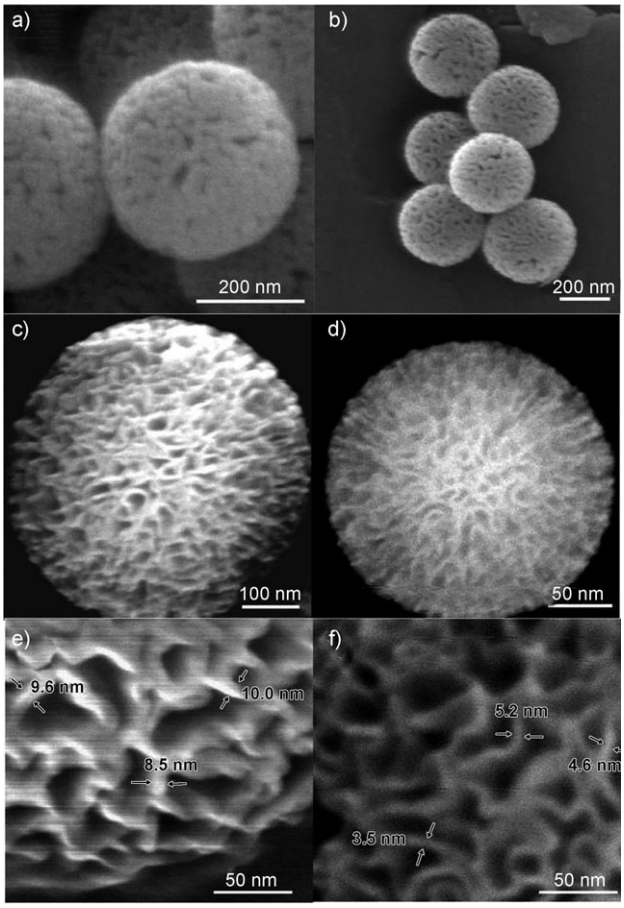

Figure 6. SEM images after calcination at a) 400 °C/6 h, b) 550 °C/6 h, c) 800 °C/6 h, and d) up to 950 °C. e,f) Fiber thickness e) before and f) after calcination.

the important condition for catalysts operating in highly exothermic media. Notably, the thickness of the fibers reduced from 8–10 nm before calcination (Figure 6e) to 4–5 nm after calcination at 550 °C (Figure 6f), which may have been due to the loss of the template coating around the fibers. This was also evident as no further reduction in the thickness or the distance between two fibers was observed, even with an increase in the calcination temperature up to 950 °C, while the microstructure of the silica remained intact. This may make it possible to prepare easily accessible catalysts in the fibrous channels of these silica nanospheres (Supporting Information, Figure S4).

The mechanical stability of the silica spheres was also examined using HRTEM. The fibrous morphology of KCC-1 remains unaffected even after mechanical compression up to 216 MPa pressure (Figure 7a–c), which is comparable to

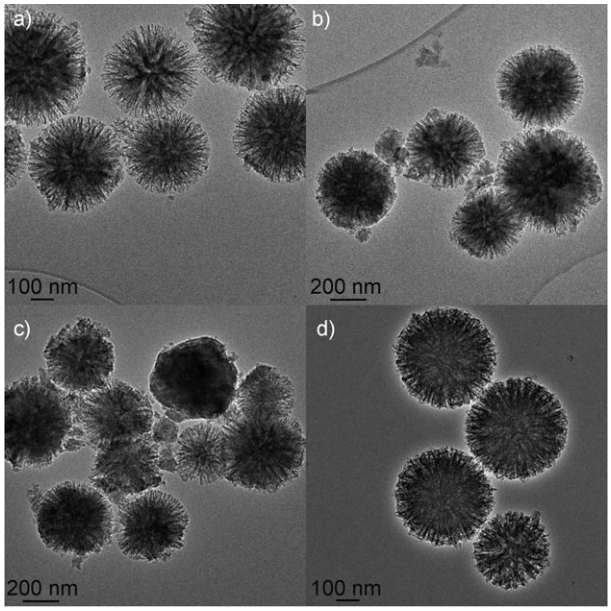

Figure 7. HRTEM images of KCC-1 after mechanical compression at pressures of a) 43 MPa, b) 130 MPa, c) 216 MPa, and d) after heating in boiling water for 24 h.

MCM-41, which is affected at pressure 86 MPa.[37] Thus, KCC-1 possesses good mechanical stability, which means that breaking of the nanospheres leading to plugging of the catalytic bed can be avoided. KCC-1 also possesses high hydrothermal stability, and even after heating in boiling water for 24 h, the fibrous morphology remained unchanged (Figure 7d). Thus, as-synthesized high-surface-area silica nanospheres have significant thermal, mechanical, and hydrothermal stabilities, which are essential attributes for good catalytic support.

In summary, we discovered a new family of high-surface-area silica nanospheres with unprecedented fibrous morphologies. The material exhibits excellent physical properties, including a high surface area, a fibrous surface morphology, good thermal and hydrothermal stabilities, and high mechanical stability. KCC-1 will be very useful for silica-supported catalysts, wherein accessibility of active sites can be increased significantly. It can also be valuable in drug delivery, hydrogen storage, as a chromatography support, and in nanocomposite materials.

Received: June 7, 2010
Revised: June 28, 2010
Published online: August 2, 2010

Keywords: catalyst supports · nanoparticles · nanostructures · silicon dioxide

[1] B. G. Trewyn, S. Giri, I. I. Slowing, V. S. Y. Lin, *Chem. Commun.* **2007**, 3236–3245.
[2] Y. Xia, B. Gates, Y. Yin, Y. Lu, *Adv. Mater.* **2000**, *12*, 693–713.
[3] J. L. Gole, Z. L. Wang, Z. R. Dai, J. Stout, M. White, *Colloid Polym. Sci.* **2003**, *281*, 673–685.
[4] T. Kusamoto, J. Ruiz, D. Astruc, *New J. Chem.* **2009**, *33*, 2204–2207.
[5] C. T. Kresge, M. E. Leonowicz, W. J. Roth, J. C. Vartuli, J. S. Beck, *Nature* **1992**, *359*, 710–712.
[6] Q. Huo, D. I. Margolese, U. Ciesla, P. Feng, T. E. Gier, P. Sieger, R. Leon, P. M. Petroff, F. Schüth, G. D. Stucky, *Nature* **1994**, *368*, 317–321.
[7] P. T. Tanev, T. J. Pinnavaia, *Science* **1995**, *267*, 865–867.
[8] D. Zhao, J. Feng, Q. Huo, N. Melosh, G. H. Fredrickson, B. F. Chmelka, G. D. Stucky, *Science* **1998**, *279*, 548–552.
[9] A. Carlsson, M. Kaneda, Y. Sakamoto, O. Terasaki, R. Ryoo, S. H. Joo, *J. Electron Microsc.* **1999**, *48*, 795–798.
[10] J. N. Cha, G. D. Stucky, D. E. Morse, T. J. Deming, *Nature* **2000**, *403*, 289–292.
[11] Y. Sakamoto, M. Kaneda, O. Terasaki, D. Y. Zhao, J. M. Kim, G. Stucky, H. J. Shin, R. Ryoo, *Nature* **2000**, *408*, 449–453.
[12] Y. Lu, Y. Yang, A. Sellinger, M. Lu, J. Huang, H. Fan, R. Haddad, G. Lopez, A. R. Burns, D. Y. Sasaki, J. Shelnutt, C. J. Brinker, *Nature* **2001**, *410*, 913–917.
[13] A. C. Finnefrock, R. Ulrich, A. D. Chesne, C. C. Honeker, K. Schumacher, K. K. Unger, S. M. Gruner, U. Wiesner, *Angew. Chem.* **2001**, *113*, 1247–1251; *Angew. Chem. Int. Ed.* **2001**, *40*, 1207–1211.
[14] C. Z. Yu, B. Z. Tian, J. Fan, G. D. Stucky, D. J. Zhao, *J. Am. Chem. Soc.* **2002**, *124*, 4556–4557.
[15] S. Che, A. E. Garcia-Bennett, T. Yokoi, K. Sakamoto, H. Kunieda, O. Terasaki, T. Tatsumi, *Nat. Mater.* **2003**, *2*, 801–805.
[16] S. Che, Z. Liu, T. Ohsuna, K. Sakamoto, O. Terasaki, T. Tatsumi, *Nature* **2004**, *429*, 281–284.
[17] T. Yokoi, Y. Sakamoto, O. Terasaki, Y. Kubota, T. Okubo, T. Tatsumi, *J. Am. Chem. Soc.* **2006**, *128*, 13664–13665.
[18] C. Gao, Y. Sakamoto, K. Sakamoto, O. Terasaki, S. Che, *Angew. Chem.* **2006**, *118*, 4401–4404; *Angew. Chem. Int. Ed.* **2006**, *45*, 4295–4298.
[19] Z. Bao, M. R. Weatherspoon, S. Shian, Y. Cai, P. D. Graham, S. M. Allan, G. Ahmad, M. B. Dickerson, B. C. Church, Z. Kang, H. W. Abernathy III, C. J. Summers, M. Liu, K. H. Sandhage, *Nature* **2007**, *446*, 172–175.
[20] Y. Han, D. Zhang, L. L. Chng, J. Sun, L. Zhao, X. Zou, J. Y. Ying, *Nat. Chem.* **2009**, *1*, 123–127.
[21] K. Suzuki, S. Sato, F. Makoto, *Nat. Chem.* **2009**, *1*, 1–5.
[22] Z. Meng, C. Xue, Q. Zhang, X. Yu, K. Xi, X. Jia, *Langmuir* **2009**, *25*, 7879–7883.
[23] M. E. Davis, *Nature* **2002**, *417*, 813–821.
[24] A. Corma, H. Garcia, *Top. Catal.* **2008**, *48*, 8–31.
[25] B. M. Weckhuysen, *Nat. Chem.* **2009**, *1*, 690–691.
[26] A. J. Gellman, N. Shukla, *Nat. Mater.* **2009**, *8*, 87–88.

[27] G. J. Hutchings, *J. Mater. Chem.* **2009**, *19*, 1222 – 1235.
[28] S. H. Joo, J. Y. Park, C. K. Tsung, Y. Yamada, P. Yang, G. A. Somorjai, *Nat. Mater.* **2009**, *8*, 126 – 131.
[29] R. Schlögl, S. B. A. Hamid, *Angew. Chem.* **2004**, *116*, 1656 – 1667; *Angew. Chem. Int. Ed.* **2004**, *43*, 1628 – 1637.
[30] "Size-selective synthesis of nanostructured metal and metal oxide-colloids and their use as catalysts": M. T. Reetz in *Nanoparticles and Catalysis* (Ed.: D. Astruc), Wiley-VCH, Weinheim, **2008**, pp. 255 – 279.
[31] a) V. Polshettiwar, B. Baruwati, R. S. Varma, *ACS Nano* **2009**, *3*, 728 – 736; b) V. Polshettiwar, R. S. Varma, *Green Chem.* **2010**, *12*, 743 – 754; c) V. Polshettiwar, B. Baruwati, R. S. Varma, *Chem. Commun.* **2009**, 1837 – 1839; d) V. Polshettiwar, R. S. Varma, *Chem. Eur. J.* **2009**, *15*, 1582 – 1586; e) V. Polshettiwar, M, Nadaguada, R. S. Varma, *Chem. Commun.* **2008**, 6318 – 6320.
[32] P. Avenier, M. Taoufik, A. Lesage, X. Solans-Monfort, A. Baudouin, A. de Mallmann, L. Veyre, J.-M. Basset, O. Eisenstein, L. Emsley, E. A. Quadrelli, *Science* **2007**, *317*, 1056 – 1060.
[33] V. Vidal, A. Théolier, J. Thivolle-Cazat, J. M. Basset, *Science* **1997**, *276*, 99 – 102.
[34] V. Polshettiwar, J. M. Basset, High-Surface-Area Fibrous Silica Nanoparticles. US patent provisional application, 61/309,721, **2010**.
[35] D. Volkov, J. Benson, Y. Kievsky, I. Sokolov, *Phys. Chem. Chem. Phys.* **2010**, *12*, 341 – 344, and references therein.
[36] Q. S. Huo, D. I. Margolese, G. D. Stucky, *Chem. Mater.* **1996**, *8*, 1147 – 1160.
[37] V. Yu, G. X. Feng, Z. Bu, G. L. Haller, J. A. O'Brien, *J. Phys. Chem.* **1996**, *100*, 1985 – 1988.

